Cationic silver enhances the rate of cyclobutane pyrimidine dimer formation by increasing intersystem crossing

A Senior Honors Thesis

Presented in Partial Fulfillment of the Requirements for graduation *with research distinction* the undergraduate colleges of The Ohio State University

by

Javad Raymond Azadi

The Ohio State University
June 2009

Project Advisor: Professor Bern Kohler, Department of Chemistry

Acknowledgements

I would like to thank the following people for their help and guidance during these past four years of undergraduate research at The Ohio State University: Professor Bern Kohler, Dean Terry Gustafson, Professor Venkat Gopalan, Mr. Yu Kay Law, Mr. Marc Coons, Mr. Joe Henrich, Mrs. Kimberly de La Harpe, and Ms. Nicole Dickson. Without their support, this thesis would not have been possible.

Abstract

DNA can undergo mutations upon exposure to ultraviolet light; if left unrepaired, these mutations may lead to cancer. Irradiation studies have shown that the primary photoproduct formed between adjacent thymine bases is the cyclobutane pyrimidine dimer. In DNA base multimers, this photoreaction occurs within one picosecond of photoexcitation; if the photoexcited thymine bases are not within a specified geometric conformational threshold at the instant of photoexcitation, dimerization will not occur. However, in the presence of Ag^+, the quantum yield of cyclobutane pyrimidine dimer formation increases. Emerging evidence concerning Ag^+-DNA complexes suggests that the increased quantum yield is a result of either increased intersystem crossing to form a longer lived triplet state, or DNA aggregation that increases the frequency of two thymine bases being within the conformational threshold during photoexcitation.

Ultraviolet C (UVC) steady-state irradiation experiments show that when the ratio of Ag^+ to nucleic phosphate (referred to as *r* in this work) becomes greater than 0.25, the quantum yield of dimerization in $(dT)_{18}$ increases with increasing Ag^+ concentrations. In addition, the quantum yield increases for TMP in the presence of Ag^+ (r=10), which suggests that increased intersystem crossing is responsible for this process, as TMP can only dimerize from the $^3\pi\pi^*$ state. Finally, circular dichroism (CD) measurements of $(dT)_{18}$ and various concentrations of Ag^+ show that although for r=0, 0.05, 0.10, and 0.25, $\Delta\varepsilon$ at 275 nm does not change, $\Delta\varepsilon$

decreases for r = 0.5 and 1.0, indicating that the system is becoming increasingly unstacked, which discredits an aggregation explanation.

Contents

List of Figures

List of Tables

Chapter 1
Introduction

Deoxyribonucleic acid (DNA) acts as the blueprint for both the development and the maintenance for all living organisms. Therefore, any damage to these blueprints can potentially be fatal. For example, damage in the region that encodes for p53, a tumor suppressing protein, would greatly increase the probability of cancer.[1] Of the many potential sources of DNA damage, exposure to ultraviolet (UV) radiation is increasingly becoming common across the globe. From damage in the ozone layer to the proliferation of tanning salons, humans are constantly being exposed to harmful UV radiation.[2,3] According to the American Cancer Society, over one million new cases of skin cancer will be diagnosed in 2008. In addition, melanoma represents the most common form of cancer found in young adult populations.[4]

Decades of research point to cyclobutane pyrimidine dimers (CPDs), specifically thymine dimers (T<>T), as the primary lesion formed in DNA from UV exposure.[26,27] Upon direct excitation by UV light, thymine may undergo a cycloaddition photoreaction with an adjacent thymine. This reaction occurs

within a picosecond of photoexcitation[5]; due to the short timescale of this process, if the adjacent thymine bases are not within a certain geometric threshold at the instant of photoexcitation, the reaction does not take place.[6]

1.1 Goals of this study

Although it is well known that metallic cations will affect the quantum yield of CPD formation ($\phi_{T<>T}$) in DNA systems,[7] much less is known about what causes these changes. The first system that we seek to categorize is DNA complexed with cationic silver. Some researchers have speculated that silver enhances dimerization by changing the associated intersystem crossing upon photoexcitation[7], while other studies have shown that certain ratios of silver to DNA phosphate cause the DNA to aggregate.[8] Therefore, we first set out to quantify enhancements of $\phi_{T<>T}$ in the model system of 18-mer of thymidylic acid $(dT)_{18}$ by Ag^+ under steady-state UVC irradiation. To detect any structural changes in $(dT)_{18}$, circular dichroism spectroscopy can be employed to monitor DNA conformational changes. Finally, increases in intersystem crossing should be detectable by increases in quantum yield of dimerization for TMP systems containing Ag^+.

1.2 Deoxyribonucleic acid

To fully understand the results reported herein, it is important to be aware of some basic, as well as fairly advanced, concepts regarding DNA. First, we shall begin

with a brief description of the chemical makeup of DNA and the nomenclature used to represent DNA. Then, we shall examine some of the most common types of DNA damage that can disrupt this pathway.

1.2.1 Nomenclature

Deoxyribonucleic acid is composed of repeating units of 5' phosphorylated D-deoxyribose where a β glycosidic bond between the hydroxyl group on the 1' carbon of the deoxyribose and the nitrogen labeled as 1 for pyrimidines or the nitrogen labeled as 9 in purines describes the nucleoside. (See Figure 1.1) A single phosphate group attached to both the 5' end of one monomer and the 3' end of another monomer link the two units together as a polymer. Nature shows us that during nucleotide biosynthesis, the end product for DNA monomers is a high-energy nucleotide triphosphate because three phosphates are linked to the 5' end of the newly formed monomer, and the energy from this triphosphate bond powers the addition of the nucleotide monomer to the growing nucleotide polymer. This explains why the 5' end of a DNA polymer will have a phosphate group, but not the 3' end. The bases can be abbreviated as A for adenine, C for cytosine, G for guanine, T for thymine and U for uracil. For example, when a sequence such as d(TT) is written, is to be understood that this represents a 2 unit DNA molecule made of thymine. [9]

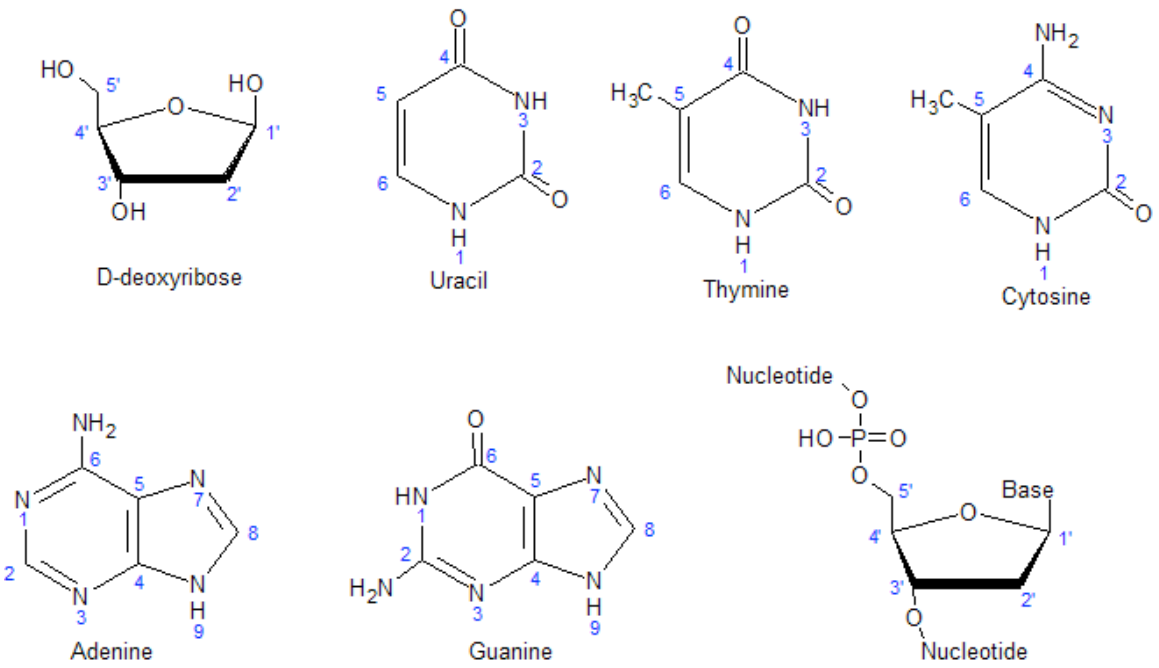

Figure 1.1: Deoxyribose, the five naturally occurring nucleic bases, and an example of connectivity in polymer form.

1.2.2 Common forms of DNA damage

Although cyclobutane pyrimidine dimers between two adjacent thymine bases are the most prominent form of damage to an organism's DNA from ultraviolet light,[10] it is not the only form of damage that can affect the vitality of said organism. Cytosine-cytosine and cytosine-thymine dimers also can occur upon photoexcitation, but much less frequently than thymine dimers. These mutations all affect DNA's ability to base pair effectively, which interferes with both DNA replication and transcription. [9]

Chemical mutagens may cause either point mutations or insertion/deletion mutations. A point mutation may occur in the form of a transition error – a pyrimidine such as thymine is substituted by another pyrimidine such as cytosine,

similarly a purine for another purine – or in the form of a transversion error – a pyrimidine is replaced by a purine, or vice-versa. Point mutations arise when the chemical mutagen directly alters a DNA base. Examples (See Figure 1.2) of chemical mutagens that induce point mutations include nitrous acid, which can deaminate bases like cytosine and adenine to form uracil and hypoxanthine, respectively, and nitrogen mustard, which can alkylate DNA to generate transversions.

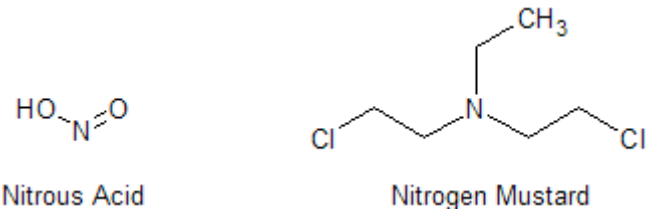

Figure 1.2: Example substances that induce point mutations.

Insertion/deletion mutations cause nucleotides to be either deleted or added which has a potential to alter the amino acid being described by the triplet codon during transcription. Insertion/deletion mutations arise when DNA is exposed to intercalating agents. Intercalating agents like acridine orange or ethidium bromide (Figure 1.3) will affect the twist angle of the DNA at the point where the agent intercalates with the DNA, and this causes the bases to separate far enough such that it is possible to fit in a new base pair during replication.[9]

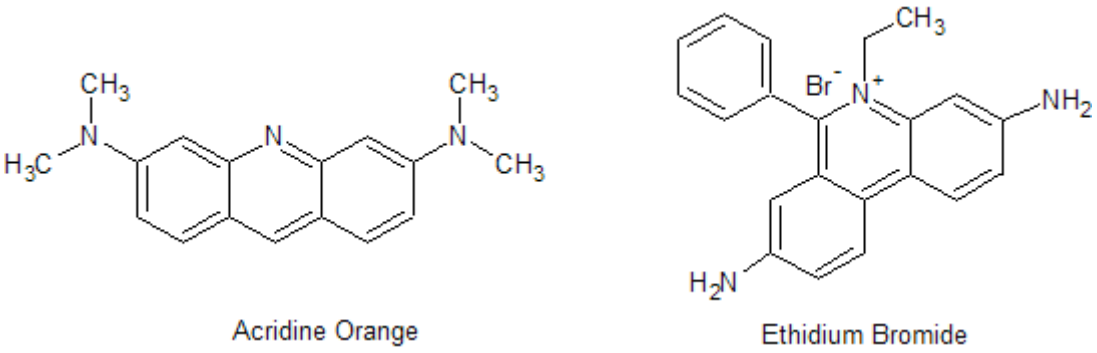

Figure 1.3: Example substances that induce insertion/deletion mutations.

1.3 Hypothesis

Our hypothesis is that cationic silver will enhance the rate of dimerization in $(dT)_{18}$ by increasing the quantum yield of intersystem crossing from the relatively short lived $^1n\pi^*$ state to the much longer lived $^3\pi\pi^*$ state. We know that increasing the concentration of Ag^+ will increase the quantum yield of dimerization in $(dT)_{18}$, but the decreasing $\Delta\varepsilon$ at 275 nm as Ag^+ is added to $(dT)_{18}$ suggested that oligomers are destacked by the Ag^+. Destacking is known to decrease the quantum yield of dimerization,[6] but when DNA is exposed to UVC light in the presence of Ag^+, when the ratio of Ag^+ to phosphate groups in DNA is greater than 1/4, the yield actually increases. This paradoxical increase in dimer yield can be attributed to an increase in intersystem crossing. In addition, unlike the oligomer systems of thymidylic acid, the dimerization of the monomer thymidine monophosphate (TMP) is diffusion-controlled, and because the $^1\pi\pi^*$ state decays faster than TMP can find another TMP, the reaction must be dependent on the $^3\pi\pi^*$ state. Therefore, because the dimer yield increases for TMP in the presence of Ag^+ when

exposed to UVC compared to just TMP alone, this also strongly suggests that Ag^+ increases intersystem crossing in photoexcited thymine.

1.4 Review of current theory

Over the past decade, an explosion in scholarship has emerged which gives a clearer understanding to how two adjacent thymine bases can form dimers upon photoexcitation. First, we shall examine the advances in photochemical understandings of thymine dimerization, and we shall discuss the current theories in thymine photophysics. Finally we shall conclude with a discussion of the works investigating the interactions of cationic silver with DNA.

1.4.1 Photochemistry

Thymine dimerization as a photoreaction involves the [2+2] cycloaddition of the C5C6 double bond of one thymine base with the C5C6 double bond of an adjacent thymine base.[11] Although this cycloaddition can form various thymine dimer stereoisomers as dictated by the conformation of the thymine bases prior to cycloaddition, the *cis-syn* stereoisomer appears more frequently than the *trans-syn* stereoisomer.[6]

It is important to note that upon photoexcitation, other photoproducts may also form between adjacent thymine bases, specifically the 6-4 photoadduct and the Dewar photoproduct, which is formed upon photoexcitation of the 6-4 photoadduct (Figure 1.4).[11]

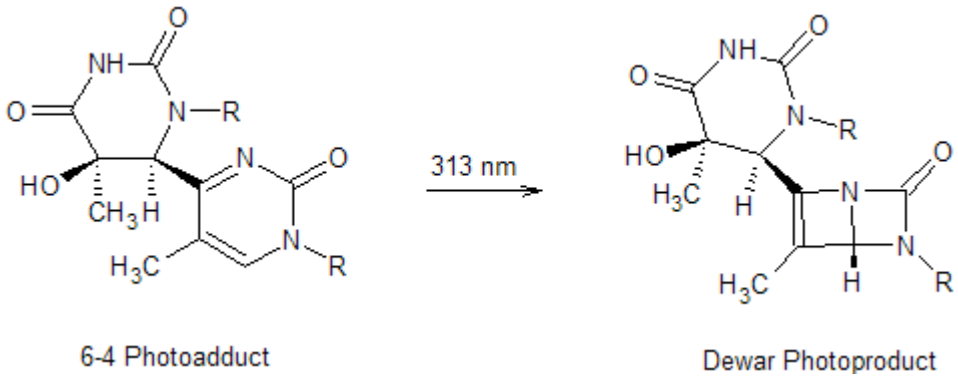

Figure 1.4: Conversion of 6-4 photoadduct to Dewar photoproduct.

Schreier et al. (2007) showed using femtosecond infrared spectroscopy that thymine dimerization in $(dT)_{18}$ is an ultrafast phenomenon that occurs within one picosecond of photoexcitation. The implications of this finding were profound in understanding how dimers form in base multimers because the photoexcited molecule would decay back to the ground state faster than the time it would take for the molecule to move. Therefore, it would appear that dimerization is controlled primarily by ground state geometric constraints. In addition, the very small quantum yield points to a conformational space that is rarely encountered.[5]

Evidence from solid-state studies of thymine dimerization also point toward a geometric criteria in order for the photoreaction take place. In ice, thymine dimers form in DNA systems with a quantum yield of approximately unity when exposed to UV light.[13] In addition, work performed by Coons et al. shows that when dTpdT systems are held in sugar glasses and undergo steady-state UVC irradiation, the dimerization yield is also near unity.[14] These various solid-state studies suggest that the compaction that occurs in the DNA from being suspended

in a matrix would greatly increase the probability of two adjacent thymines being within the necessary conformational threshold for dimerization upon photoexcitation.

Earlier work by Law et al. (2008) used molecular dynamics simulations to extrapolate the geometric threshold required for thymine dimerization to take place upon photoexcitation. Using the model system thymidylyl-(3'-5')-thymidine (dTpdT), molecular dynamics simulations in various co-solvents were examined to map out the probability of being in various confirmations. Also, work by Olmon et al. (2005) showed that increasing the organic:aqueous solvent ratio decreases the dimerization yield in $(dT)_{18}$. This effect was explained by the theory that organic solvents form hydration shells around the hydrophobic bases, which would cause the 18-mer to further destack. The same co-solvents examined by Olmon et al. were used for the simulations, and unsurprisingly, the conformational probability maps show that the solvents decrease the degree of base stacking in dTpdT. Experimentally through steady-state UVC experiments, the quantum yields of dimerization for dTpdT dissolved in aqueous solution, 40% (v/v) ethanol, 50% (v/v) dioxane, and 60% (v/v) ethanol was determined: 0.016±0.003, 0.011±0.001, 0.007±0.002, and 0.007±0.001, respectively. In addition, the quantum yield for the formation of the 6-4 photoadduct was shown to be an order of magnitude lower than the quantum yield of dimerization.[6]

Earlier studies have shown that thymine dimerization depended upon the torsional angle formed between the C5C6 double bonds,[15] and the need for a certain interbase distance between C5C6 double bonds. Using the known quantum yield of dimerization, the torsional angle formed between the C5C6-C6C5 of two adjacent thymines, defined as η, and the distance between the double bonds, it was possible to map and find a common η and double bond separation that could accurately reproduce the quantum yields of dimerization in all four systems. This geometric threshold required for dimerization upon photoexcitation between two adjacent thymine bases was determined to be $|\eta| \leq 48.2\,^{\circ}$ and $d < 3.63$ Å. The organic co-solvents decreased quantum yield by decreasing the frequency that this angle and base separation condition could be met. [6]

Systems like dTpdT and $(dT)_{18}$ have quantum yields of dimerization around 1 to 3 percent in aqueous solutions. Although dimerization is a very rare reaction by itself, when compared to the quantum yield of dimerization for TMP systems, the aforementioned percentages seem quite large. This is due to the inherent geometric constraints faced by oligomeric systems due to their connectivity by the phosphate backbone, because it becomes much more probable to encounter the dimerization threshold when in a polymer than for two free thymidines to encounter one another. However it is important to note that because there is a diffusion-constraint for dimerization in TMP, the necessary molecular motion dictates that the ultrafast $^{1}\pi\pi^{*}$ state cannot be responsible. Instead, the energy for the cycloaddition likely emerges from the much longer lived $^{3}\pi\pi^{*}$ state.

1.4.2 Photophysics

When a photon with a wavelength of 265 nm encounters a molecule of $(dT)_{18}$, it is absorbed by the system and an electron in the ground state (S0) is excited to the $^1\pi\pi^*$ excited state. However, the pathway the electron takes to return to the ground state is much more complicated than simply the electron returning directly to S0 by emitting a photon through fluorescence or phosphorescence.

Hare et al. (2007) demonstrated that for pyrimidine bases, the electron is able take one of two distinct pathways for internal conversion (IC) to the ground state. It was shown that at least 98% of all excited pyrimidine bases will decay without radiation, and that the ultrafast decay to the ground state is a result of IC within the base.[16] IC directly from the $^1\pi\pi^*$ to the ground state cannot account for 100% of the decay, however, because there is the possibility for the photoexcited molecule to undergo a chemical reaction as well. Hare et al. (2007) were able to determine using femtosecond transient absorption spectroscopy that within the first picosecond of excitation, the energy will decay via one of two pathways.[17]

Pecourt et al. (2000) proposed the first decay pathway from the $^1\pi\pi^*$ state to S0 by IC in DNA systems. For thymidine, they were able to show using femtosecond transient absorption measurements that the system returned to S0 after only 580±50 fs of photoexcitation at 265 nm. By pumping with 265 nm light at t = 0, a 600 nm probe could detect the formation and decay of the radiative energy state, that was assigned as the $^1\pi\pi^*$ state.[18]

Returning to Hare's work in 2007, the second pathway for IC that may take place involves a dark-state intermediate. Instead of decaying from $^1\pi\pi^*$ directly to S0, the energy dissipates by IC to the $^1n\pi^*$ state, which further undergoes IC to S0. This decay channel was shown to account for between 10-50% of all IC in pyrimidine. By pumping the various pyrimidine systems with 265 nm light at t=0, a 340 nm probe could detect the formation and decay of both the $^1\pi\pi^*$ and the $^1n\pi^*$ states. For TMP, the lifetimes of the $^1\pi\pi^*$ and $^1n\pi^*$ were shown to be 0.41 and 127 ps, respectively. This longer-lived $^1n\pi^*$ state is thought be associated with the formation of the 6-4 photoadduct, because just as the $^1n\pi^*$ lifetime is longer in cytosine compared to thymine, so is the yield of 6-4 photoproduct in cytosine compared to thymine.[17]

Because direct intersystem crossing from $^1\pi\pi^*$ to $^3\pi\pi^*$ is unlikely to take place,[25] Hare et al. proposed that ISC takes place by decaying from $^1\pi\pi^*$ to $^1n\pi^*$, and then from $^1n\pi^*$ the system can decay to form $^3\pi\pi^*$.[17] By pumping at 265 nm at t=0, a 450 nm probe is able to detect the formation of the rare $^3\pi\pi^*$. The lifetime of the $^3\pi\pi^*$ state was shown to be over a nanosecond in protic solvents.[19]

Radiationless decays, like the two channels mentioned above, occur via conical intersections. Using computational studies, Perun et al. were able to show that theoretically there are three intersections of the potential energy surfaces of the $^1\pi\pi^*$ state to S0. These intersections permit a molecule in the excited state to return to the ground state by expelling the energy through molecular motion

rather than radiation. Not surprisingly, the lowest energy conical intersection was found where $^1\pi\pi^*$ crosses to So, which explains why this transition is also the most common channel of internal conversion observed in pyrimidine systems.[20]

When oligomeric DNA systems containing purines are in a properly stacked confirmation, it has been shown that the decay channel for returning to So changes compared to the decay channels mentioned above. It is believed that through base stacking, π orbital overlap leads to the formation of an excimer/exciplex structure within a picosecond of photoexcitation. This excimer/exciplex may live between 3 to 200 ps before returning to the ground state.[21]

1.4.3 Interaction of cationic silver with DNA

Rahn et al. performed some of the earliest work in characterizing heavy atom complexes of DNA. Some of the questions that arose from this early work spurred the research contained within this thesis. When varying the pH, it was shown that at an acidic pH, the percentage of thymine dimers as determined by the acid hydrolysation of irradiated samples shows that Ag^+ has no effect. At neutral and basic pHs, however, the same acid hydrolysation reveals that Ag^+ increases the percentage of dimers formed. In addition, Rahn et al. explored luminescence of Ag^+ complexes with poly(dT) at 77 K, and their findings suggested that the increase in dimerization may be a result of increased triplet formation. In the DNA systems containing Ag^+, the intensity of phosphorescence was shown to

increase 20-fold compared to DNA without Ag^+. Increases in phosphorescence and increases in dimerization led Rahn et al. to speculate that increases in triplet formation were the cause. However, when comparing the rate increases from Ag^+ with other types of dimerization enhancers that transfer the triplet energy, like acetone, it would be expected that triplet sensitizers should offer greater dimerization enhancements over Ag^+, however Rahn et al. showed that this was not the case.[7]

Based on the current photochemical theories, an increase in base stacking of DNA should increase the probability of photoexcited thymine to be in a chemically reactive conformation with an adjacent thymine. Similarly, DNA aggregation has also been shown to increase dimerization yields,[11] likely because it forces the adjacent thymine bases into favorable conditions for dimerization. Therefore, when Zinchenko et al. proposed that Ag^+ can cause DNA to aggregate, this indirectly gave new insight as to how Ag^+ may increase the quantum yield of dimerization. In the work, long strands of duplex DNA were mixed with increasing concentrations of $AgNO_3$. Taking advantage of fluorescence microscopy imaging techniques, Zinchenko et al. were able to determine that without Ag^+, the average coil length was approximately 3 μm, and that as the concentration of Ag^+ increased, the average coil length decreased to approximately 1.5 μm. This is because, heavy atom metals like Ag^+ will actually intercalate between the bases, unlike standard alkali metals that simply act as counter ions to the negatively charged phosphate backbone. The effects of metallic Ag on the

DNA structure were even more pronounced. Using $NaBH_4$ to reduce the Ag^+ cations to Ag, nanoparticles of Ag were intercalated, and the average coil length fell from 3.0 μm to 0.5 μm.[8]

This intercalating nature of Ag+ is a result of the cation's ability to bind with the DNA. Arakawa et al. (2001) determined a great deal of information regarding the binding of Ag+ to DNA by utilizing Fourier Transform Infrared Spectroscopy and Capillary Electrophoresis. Although it has long been known that silver forms three types of complexes with DNA depending on the ratio of Ag+ to the phosphate moiety, little was known about the actual binding affinity. The results showed that for Type I complexes, when *r* is around 1/80, Ag^+ interacts with guanine N7, and when *r* increases to around 1/20, Ag^+ begins to interact with adenine N7. This binding was shown using Scatchard analysis to be $K1 = 8.3 \times 10^4\ M^{-1}$ for the guanine and $K2 = 1.5 \times 10^4\ M^{-1}$. When *r* increases to approximately 0.5, Type II complexes arise due to the Ag^+ interacting between the A-T and G-C basepairs.[22]

Chapter 2
Principles of Experimental Methods

2.1 Theories of absorption spectroscopy

All of the experiments contained within this thesis deal with the manipulation of light. The fundamental definition of light is that it is actually radiation composed of oscillating electric and magnetic fields, defined as **E** and **H** respectively, that transverse along the path of the light, and the oscillations occur in phase like sine functions in perpendicular planes.[23]

The oscillations that occur per second define the ν, and the distance between two of the crests define λ. The speed of light is defined by multiplying distance between two crests by frequency of oscillations, or more simply $c = \lambda\nu$, which is approximately 3×10^8 m s^{-1} in air. [23]

Max Planck's work showed that light carries energy in discrete units that are referred to as photons. The energy is defined by the frequency of the light, and the scalar factor, h, was determined to be 6.63×10^{-34} J s, therefore $E = h\nu$. [23]

It is important to note that even though Planck showed that light behaves like a particle, it also behaves like a wave. A photon is mass-less, and it exhibits characteristics of both a wave and a particle. [23]

2.1.1 Molecular absorption

Because light is composed of oscillating electric and magnetic fields, when light passes by an atom, both electrons and protons will respond to the electric field by oscillating. Because electrons are much lighter than protons, the force felt by the electrons causes a much larger disturbance than in the heavier nucleus. This large disturbance causes the oscillating electrons act like an antenna, causing the energy from the light to be reemitted, therefore ensuring that the intensity of the light is unaffected. [23]

The situation changes when the energy of the photon is equal to the necessary energy to bridge the gap between one state and another state of an atom or molecule. When this situation is encountered, the photon is 'swallowed' by the atom, and the molecule is considered to have moved to a more excited energy state. However, this description on its own cannot explain why two molecules that absorb the same photon do so with different intensities. [23]

The difference in absorption intensities, or molar absorptivity, is explained through transition moments. During excitation, the shape of the electrons changes to that of a more excited state, and this may require a shift or rotation of

the electron charge. The transition moment vector, $\boldsymbol{\mu}_{oa}$, describes how this shift takes place. The square of $\boldsymbol{\mu}_{oa}$ defines the dipole strength, D_{oa}, and the value of D_{oa} is proportional to the absorption band. The most intense changes in dipole moment during excitation, like going from -x to x, will result in very high molar absorptivity, while if there is no change in dipole moment during excitation, the structure is considered electronically forbidden and the molar absorptivity will be approximately zero. [23]

Absorption spectroscopy relies on measuring changes in transmission. A known intensity of light at a specified wavelength, Io, travels through a sample, and if the sample absorbs light at that wavelength, then the intensity of the light will decrease to value I. This change is computed into transmission T, where T = I/Io. To convert the measured transmission to absorbance, one must simply take the negative base 10 logarithm of the transmission, or A = -log(I/Io).[24]

Absorption was shown to be proportional to both the concentration of the sample and the path length of the sample, and this relationship is known as the Beer–Lambert law, or $A = \varepsilon l c$ where ε is molar absorptivity at a particular wavelength, l is path length and c is concentration. This equation is very useful for determining concentration of an unknown solution from an absorbance, the molar absorptivity, and path length, assuming that the absorbance changes linearly with concentration. This is because absorptivity becomes unreliable when transmission is less than 10% or greater than 90% because of the logarithmic relationship. In

addition, the sample may even exhibit nonlinear response between 10% and 90% transmission if the chromophore undergoes a structural change as the concentration changes. [24]

2.1.2 Circular Dichroism

An optically active substance does not absorb left and right circularly polarized light equally, a phenomenon known as circular dichroism. This difference in absorption can be represented just like normal absorption, except $A_L = -\log (I_L/Io)$ and $A_R = -\log (I_R/Io)$ because $Io_L = Io_R = Io$. Therefore, the absorbance can be measured as $\Delta A = A_L - A_R$, thus $\Delta\varepsilon = \Delta A/(cl)$. However, since $A_L - A_R = -\log (I_L/Io) + \log (I_R/Io) = \log (I_R/I_L)$, there is no need for a reference beam because only the change in emitted intensity matters. [23]

Just as the electronic transition moment is important for absorption spectroscopy, so is the magnetic moment for circular dichroism spectroscopy. When the electron charge must rotate during excitation, the rotating charge generates a magnetic field, **m**. The magnetic moment was shown to be important for CD spectroscopy, and it is proportional to rotational strength *R*. The simplest relationship is $R = \mu_{oa} m_{oa} \cos(\boldsymbol{\mu}, \mathbf{m})$, where μ_{oa} and m_{oa} are the respective magnitudes while $\cos(\boldsymbol{\mu}, \mathbf{m})$ is simply the cosine between the two vectors. Therefore from this relationship, it can be stated that for *R* to exist there must be an electric transition moment, a magnetic transition moment, and the two

moments cannot be perpendicular. If *R* is equal to zero for a given transition, then the molecule will not exhibit circular dichroism. [23]

2.2 Qualitative relations in biochemistry

CD spectroscopy can be a very useful tool in analyzing DNA. Although DNA bases exhibit a plane of symmetry and have no optical activity on their own, the asymmetric deoxyribose can induce CD in the base's chromophores. This leads to the detection of a weak CD absorption for DNA bases. However, as DNA bases stack and the DNA forms a helical structure, the molecule becomes as a whole asymmetric, thus leading to high intensity CD absorption. This relationship has led to use of CD spectroscopy as a sensitive tool for detecting changes in DNA secondary structure. [23]

Chapter 3
Experimental methods

3.1 Steady-state irradiation

Steady-state irradiation experiments took place in Rayonet photoreactor with a single UVC G8T5 lamp. Reflective surfaces inside of the Rayonet were masked with black poster board, so that only light emitted directly from the UVC lamp will penetrate the sample. All samples were contained in a 1 cm quartz cuvette with frosted sides, which caused photons to enter the sample only through the face directly perpendicular to the light source. The cuvette was stirred by a 1x5 mm magnetic stirbar, and the cuvette was capped to keep the volume of the sample constant throughout the reaction.

Samples were prepared by dissolving lyophilized, HPLC-purified $(dT)_{18}$ (Midland Reagent, 5 U/mL) in 6.00 mL of 50 mM $NaClO_4$. All absorption measurements were made against a 50 mM $NaClO_4$ solution background. The sample was divided into two 3 mL aliquots in order to conserve limited DNA supplies, and the absorption at 265 nm of each 3 mL aliquot is determined in order to determine how many milliliters of 414 μM $AgNO_3$ were required to achieve a specified ratio of

cationic silver to the phosphate group in DNA (18 phosphate groups per molecule of $(dT)_{18}$).

To achieve desired doses of UV light, the pathway of the UVC lamp to the sample holder was obstructed by a rectangular piece of black poster board during the 1 to 3 s it took to remove the cuvette for measurements or return the cuvette for further exposure.

For $(dT)_{18}$ systems, absorption measurements from 200 to 400 nm were taken every 30 s until the sample had received a total of 5 min of irradiation, then for every 10 min interval of total irradiation until the sample had underwent 40 minutes of exposure. Said systems contained ratios of Ag^+ to nucleic phosphate, abbreviated *r*, of *r* = 0.025, 0.05, 0.10, 0.25, 0.5 and 1.0 were prepared by adding 1, 2, 4, 10, 20 and 40 µL of 414 mM $AgNO_3$ to each $(dT)_{18}$ solution.

For TMP systems, a grain-sized sample of TMP was dissolved into 50 mM NaClO4, and diluting the solution reduced the absorption until it fell within the range of 1.0 to 0.40. A system of TMP with *r* = 0 and with *r* = 10 were irradiated by UVC. Absorption measurements from 200 to 400 nm were taken after the first 5 minutes and every 10 min of total irradiation for 60 min of exposure time.

To quantify photon flux, a 1,3-dimethyluracil (DMU) actinometer was utilized. A solution of DMU was prepared by dissolving a grain-sized sample of DMU into 50 mM NaClO4, and the solution was diluted until the absorbance fell below 1.0. This solution was irradiated for 90 seconds at the same distance from the UVC lamp as

the other irradiated samples in order to accurately measure the amount of photons passing through the surface of the cuvette. The absorption at 254 nm, the mode of the UVC lamp's narrowband emission, was measured at 0 and 90 seconds, and the two absorptions could be used to calculate the photons being emitted per minute per cm^2.

3.2 CD spectroscopy

CD spectra were collected using AVIV Model 202 Circualr Dichroism Machine. All measurements were made at 25 °C, from 200 to 350 nm, at 1 nm resolution, with 2 s averaging for each nm scanned, and 3 scans averaged for each sample to produce a final spectrum. A 1 cm quartz cuvette was used to hold all samples being measured.

Before adding $AgNO_3$ to a sample for steady-state irradiation, 3 mL of (dT)18 dissolved in 50 mM $NaClO_4$ was separated for measurement using CD spectrophotometer. The absorption of the sample at 265 nm was measured in order to determine the molarity of the sample before measuring CD spectra.

A background spectrum of just 50 mM $NaClO_4$ was taken before each day of scans in order to account for any fluctuations in the light source intensity that might arise. In addition, even though the solvent solution does not absorb from 200 to 350 nm, the CD spectra will show negative absorption near the 200 nm end of the spectrum.

To ensure uniform concentration between the various $(dT)_{18}$ samples being measured, only one sample of $(dT)_{18}$ was used, and the concentration of Ag^+ was increased by pipetting $AgNO_3$ into the cuvette as necessary. Therefore, in order to measure CD spectra for r = 0, 0.025, 0.05, 0.10, 0.5 and 1.0, the sample initially did not contain Ag^+, then 1, 1, 2, 6, 10 µL, and 20 µL of 414 µM $AgNO_3$ was added to bring the Ag^+ to nucleic phosphate ratio to the desired level. The total volume of the sample was not significantly changed; the volume of the original $(dT)_{18}$ solution was approximately 3 mL and 3.04 mL after the final titration.

Using the built-in software, each averaged CD spectrum for the various systems was corrected by subtracting the solvent spectrum. By using the calculated molarity of $(dT)_{18}$ for all of the samples and the path length of the cuvette, it was also possible to use the built-in software to convert the obtained spectra from ΔA spectra into the more relevant Δε spectra.

Chapter 4
Results and discussion

All data and graphing analysis were performed using Igor Pro 6.0, and photon flux calculations were performed using Mathematica 7.0, both on the Mac OS X platform.

4.1 Steady-state irradiation

Steady-state irradiation of both $(dT)_{18}$ and TMP reveals information about the kinetics of thymine dimer formation.

4.1.1 Results

Figures 4.1-4.8 portray the decreases in absorbance at 265 nm during steady-state irradiation. Although these graphs are useful in showing the destruction of the C5C6 chromophore in thymine, they provide very little information about the actual quantum yield of the reaction. Instead, we must take advantage of knowing the photon flux through each sample.

All $(dT)_{18}$ systems exhibited similar trends in their spectra: the decreasing absorbance at 265 nm indicates the destruction of the chromophore because photoproduct is being formed, uncharacterized loss of absorbance around 220 nm,

and the increase in absorbance at 325 nm indicates the formation of the 6-4 photoadduct.

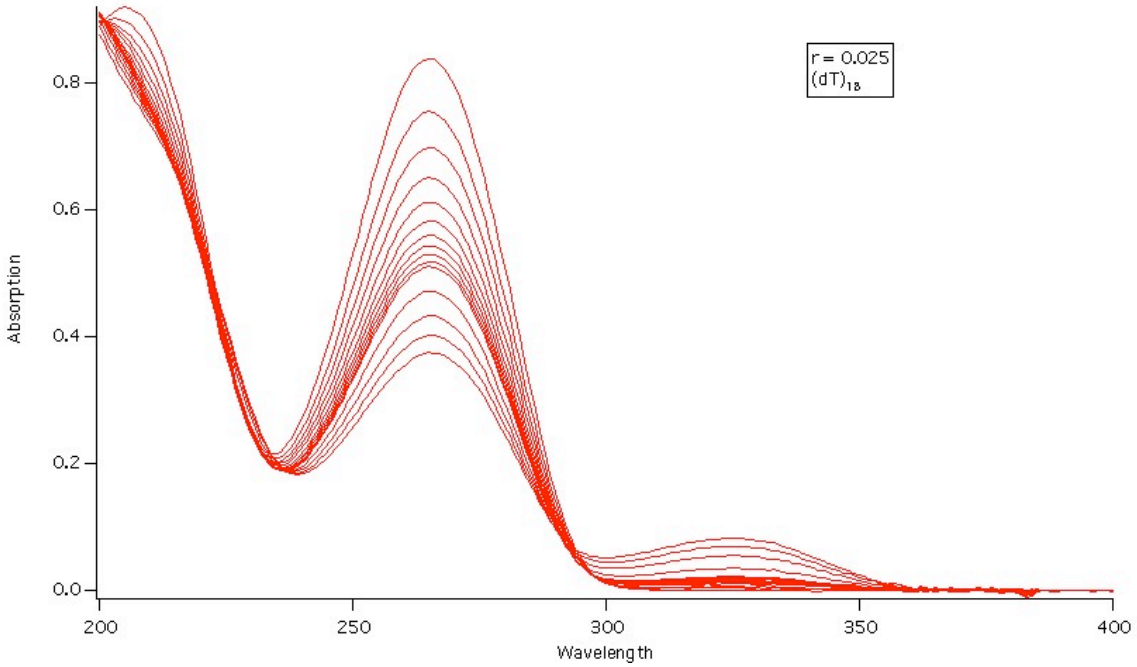

Figure 4.1: Absorption versus wavelength in nm for $(dT)_{18}$ with r = 0.025; absorbance decreases at 265 nm as irradiation time increases.

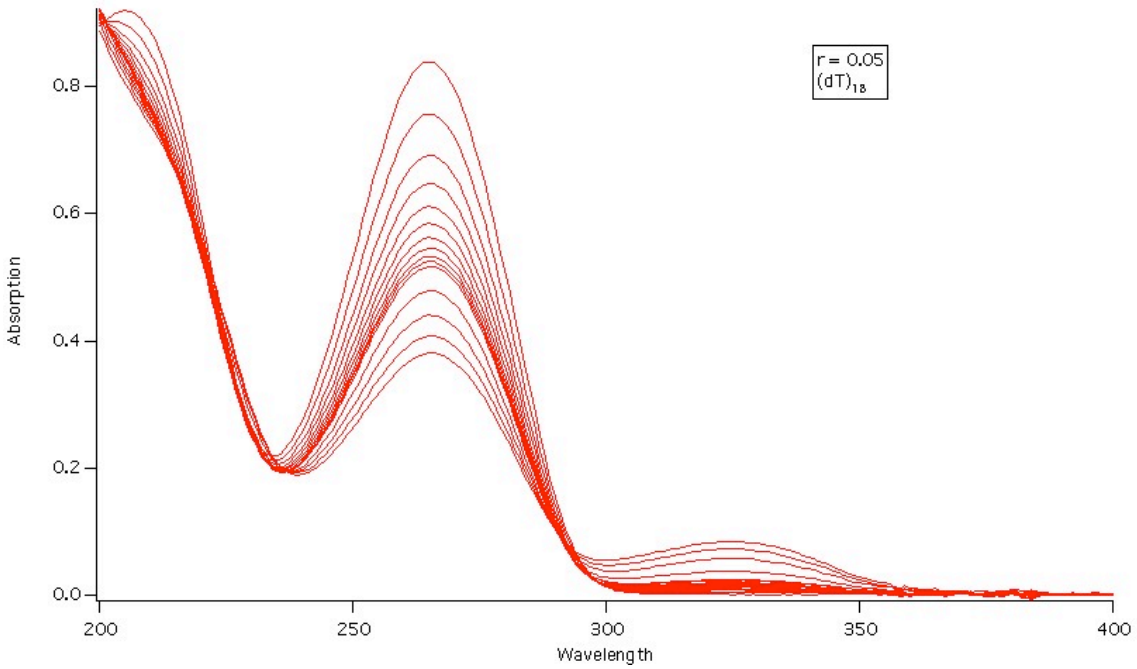

Figure 4.2: Absorption versus wavelength in nm for $(dT)_{18}$ with r = 0.05; absorbance decreases at 265 nm as irradiation time increases

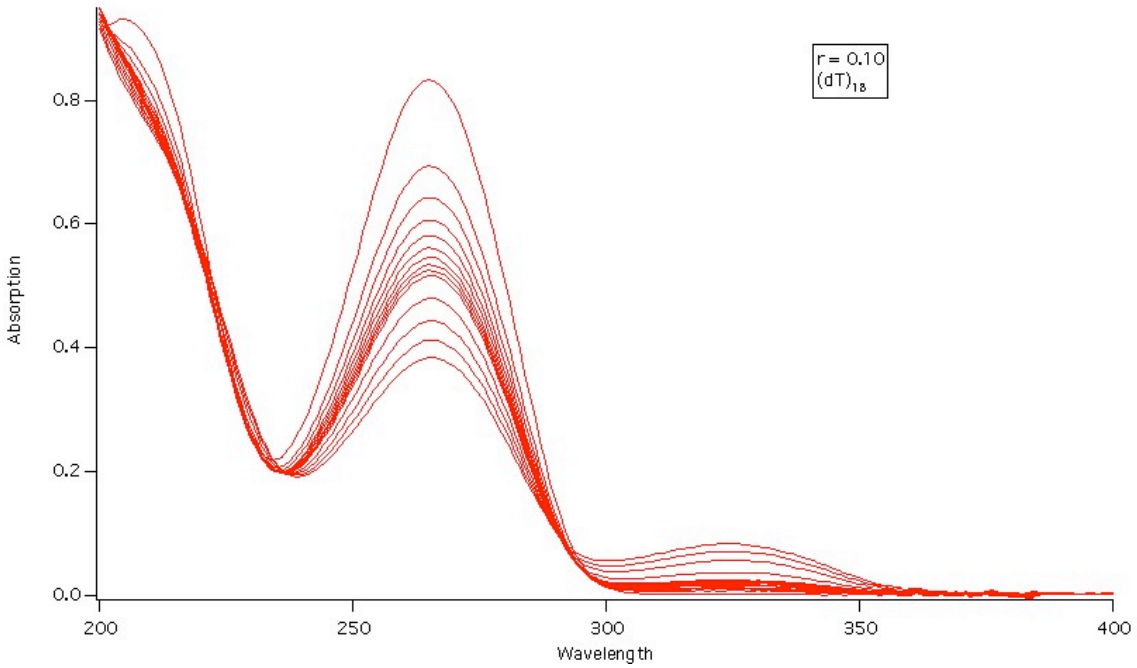

Figure 4.3: Absorption versus wavelength in nm for $(dT)_{18}$ with r = 0.010; absorbance decreases at 265 nm as irradiation time increases.

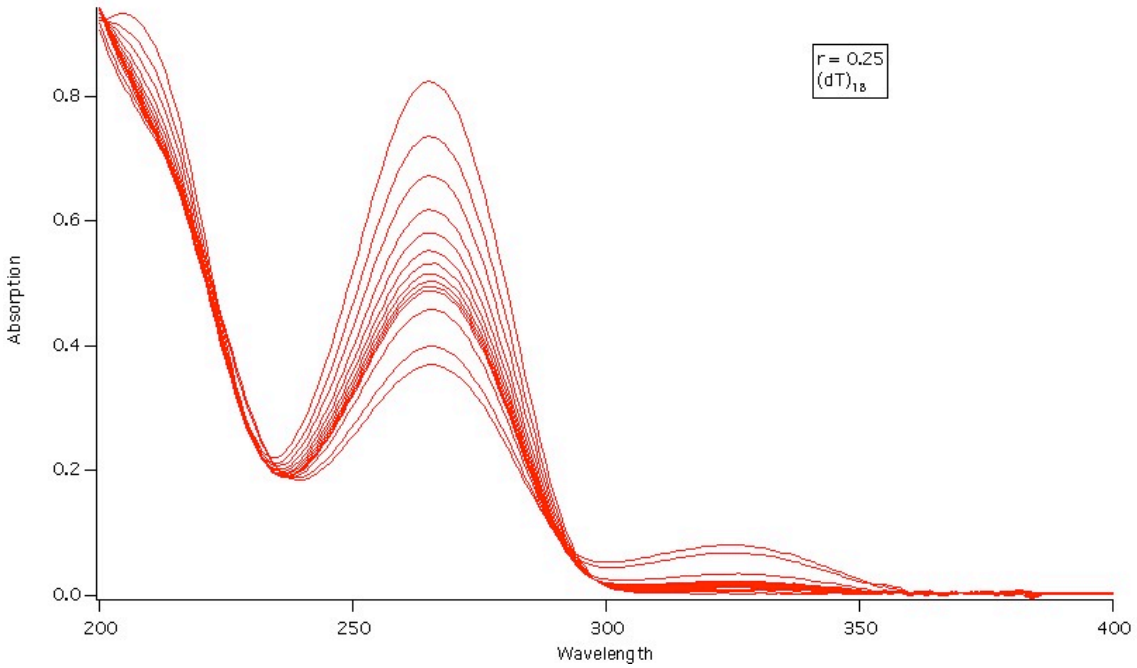

Figure 4.4: Absorption versus wavelength in nm for $(dT)_{18}$ with r = 0.25; absorbance decreases at 265 nm as irradiation time increases.

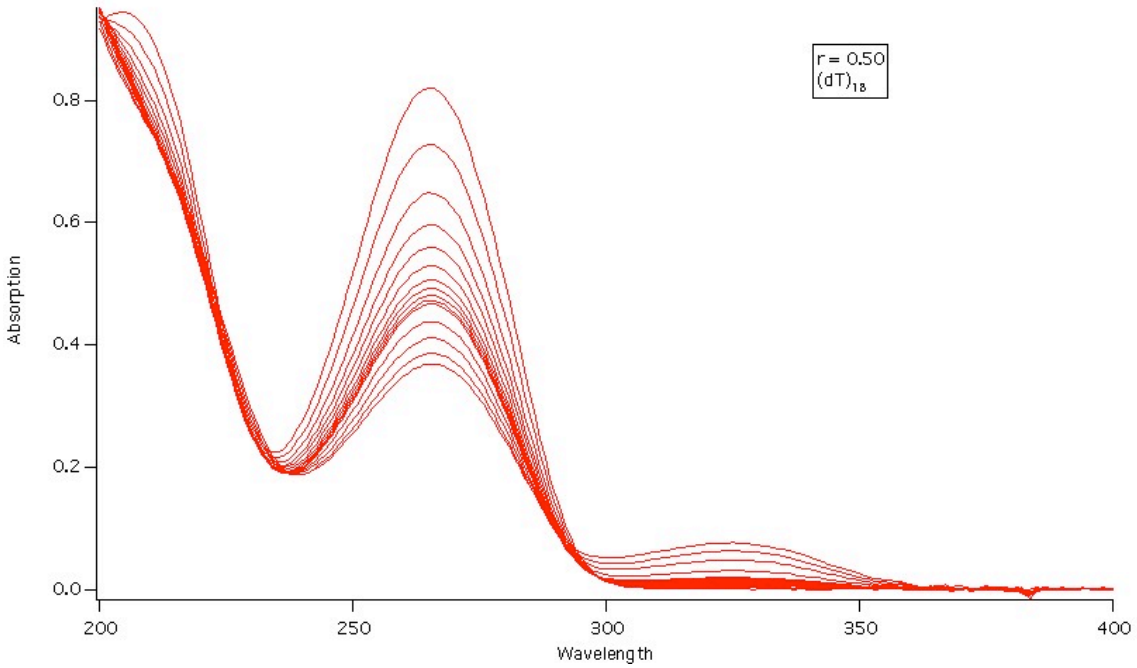

Figure 4.5: Absorption versus wavelength in nm for $(dT)_{18}$ with r = 0.50; absorbance decreases at 265 nm as irradiation time increases

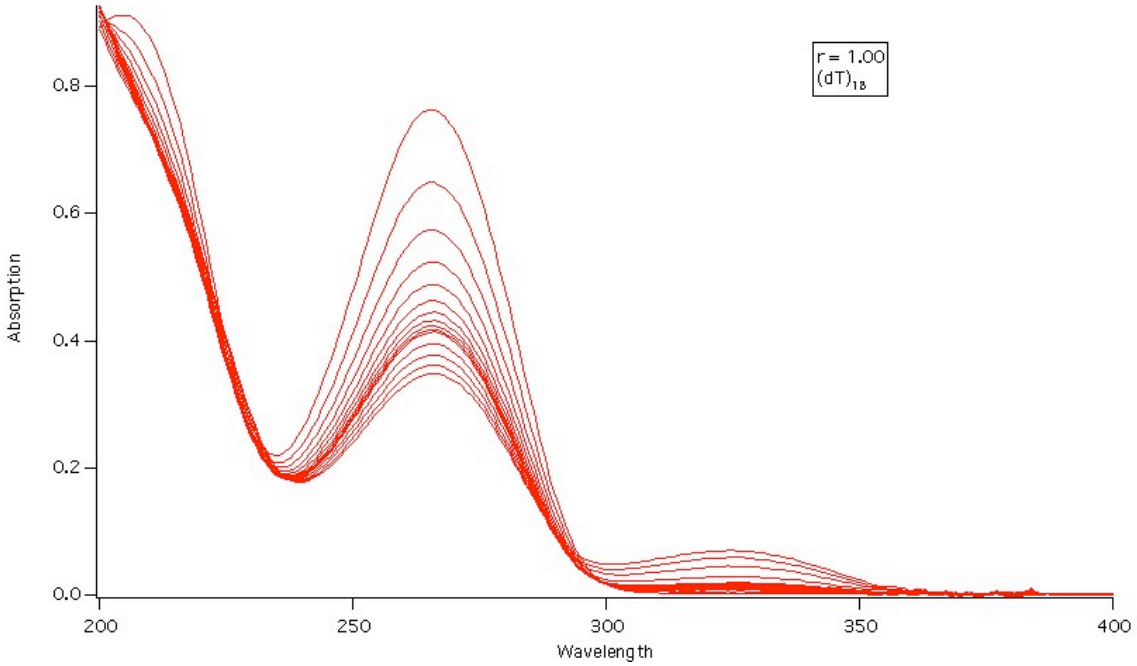

Figure 4.6: Absorption versus wavelength in nm for $(dT)_{18}$ with r = 1.00; absorbance decreases at 265 nm as irradiation time increases

TMP without Ag^+ exhibited similar trends in its spectra compared to $(dT)_{18}$, except the rate of decrease at 265 nm is much slower. TMP with r = 10 exhibits a more rapid decrease at 265 nm, but it also gains absorbance at 300 nm to 400 nm, and this absorbance increases over time.

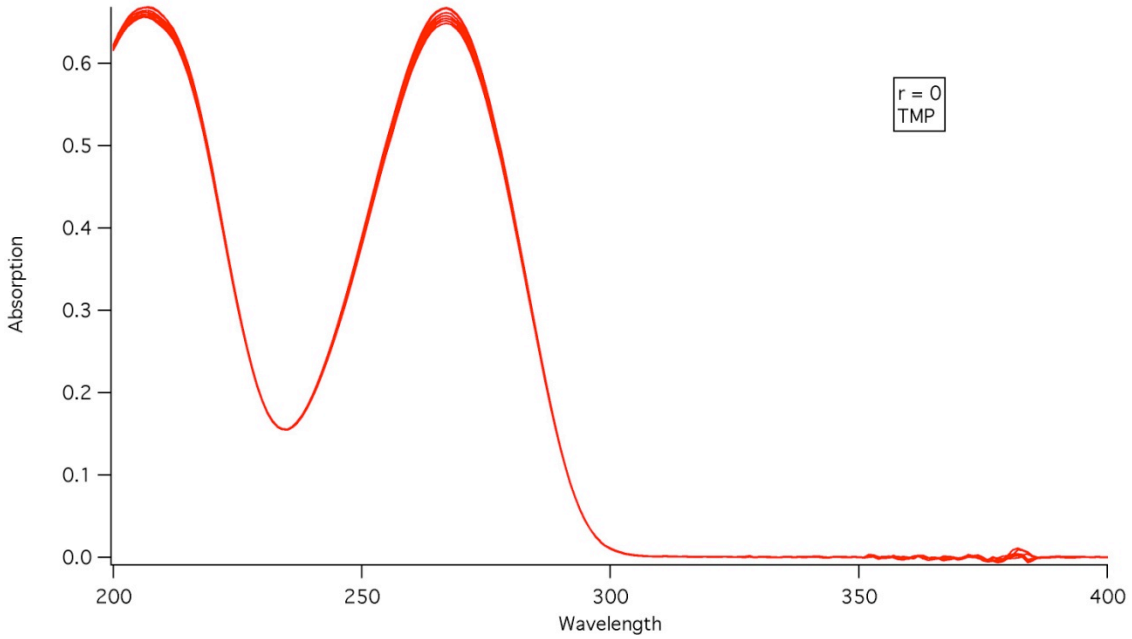

Figure 4.7: Absorption versus wavelength in nm for TMP with r = 0; absorbance decreases at 265 nm as irradiation time increases.

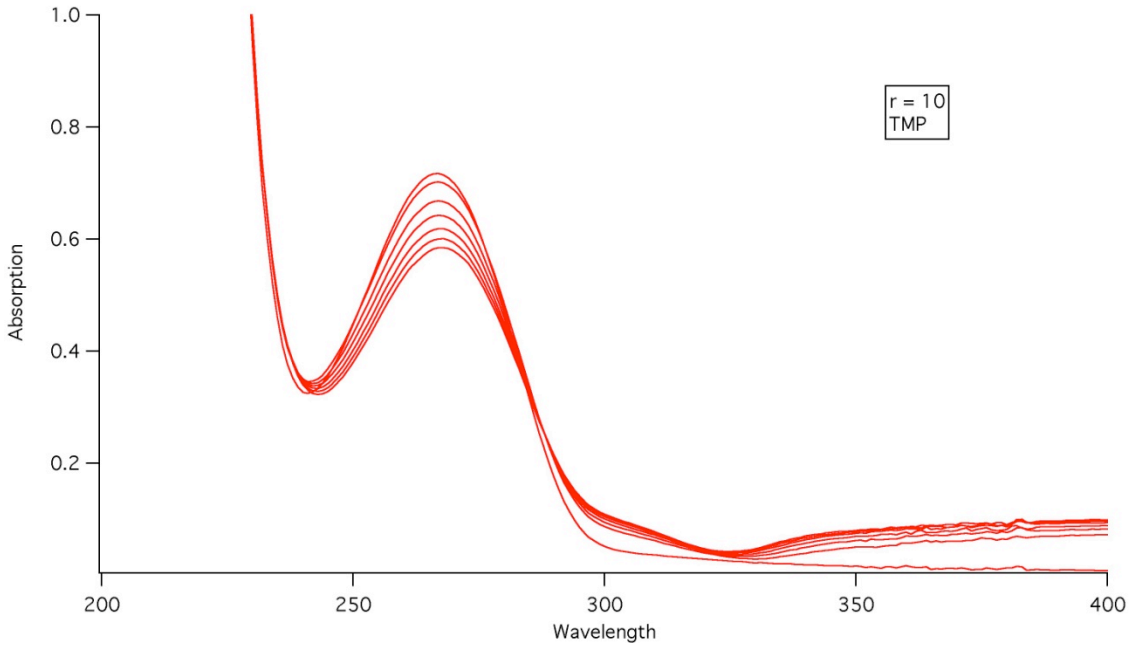

Figure 4.8: Absorption versus wavelength in nm for TMP with *r* = 10; absorbance decreases at 265 nm as irradiation time increases.

Samples of $(dT)_{18}$ with *r* = 0.025 to 0.5 were irradiated with Io = 3.97 x 10^{-7} einsteins/(min*cm²), TMP with *r* = 0 and (dT)18 with *r* = 1.00 were irradiated with Io = 3.99 x 10-7 einsteins/(min*cm²), and TMP with *r* = 1.00 was irradiated with Io = 3.73 x 10^{-7} einsteins/(min cm²). These values were calculated from the formula:

$$I_o = \frac{1}{\varepsilon_{DMU}\phi_{hyd}\Delta t \ln 10} \ln\left(\frac{e^{A_o \ln 10} - 1}{e^{A_t \ln 10} - 1}\right)$$

The total number of photons absorbed at any time by the various systems was calculated from the formula:

$$I_a = I_o \times (1 - 10^{-(A_o + A_t)/2}) \times t$$

From the absorbance at 265 nm, we are able to calculate the concentration of $(dT)_{18}$ at each time point based on the molar absorptivity of 152,150 M^{-1} cm^{-1}, as calculated by IDT using Cavaluzzi-Borer Correction.[28] Because $(dT)_{18}$ has 9 sites for potential dimer formation, we shall multiply the concentration by 9 when we are attempting to quantify dimer formation. By graphing concentration of $(dT)_{18}$ versus einsteins of photons absorbed per L of sample, we are able to fit the data points with the following function:

$$[(dT)_{18}] = [(dT)_{18}]_o + A_1 \exp(\frac{-(I_a)}{\tau_1}) + A_2 \exp(\frac{-(I_a)}{\tau_2})$$

The fit data for each $(dT)_{18}$ system are listed in table 4.1 and the fit functions are applied to each system in figure 4.9.

r	A1 x 10^{-5}	τ1 x 10^{-4}	A2 x 10^{-5}	τ2
0.025	1.99 ± 0.02	6.1 ± 0.1	4 ± 3	0.05 ± 0.06
0.05	1.91 ± 0.01	5.60 ± 0.07	2.3 ± 0.5	0.028 ± 0.008
0.10	1.88 ± 0.02	5.6 ± 0.1	3 ± 1	0.04 ± 0.02
0.25	2.03 ± 0.02	5.4 ± 0.1	0.01± 2.08 x 10^5	20 ± 4+03
0.50	2.19 ± 0.02	4.75 ± 0.06	1.5 ± 0.5	0.02 ± 0.01
1.00	2.080 ± 0.009	4.11 ± 0.03	2 ± 1	0.05 ± 0.03

Table 4.1: Parameters for double exponential fitting.

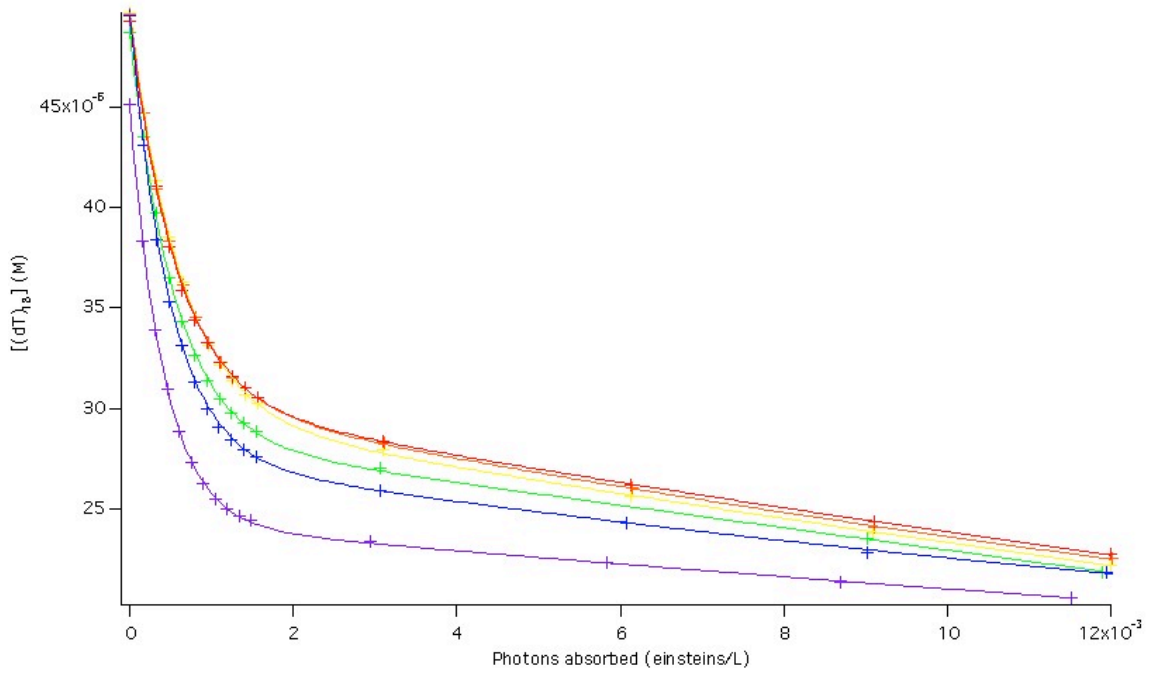

Figure 4.9: Concentration $(dT)_{18}$ versus photons absorbed, with best fit function imposed. Red – r = 0.10; Orange – r = 0.05; Yellow – r = 0.025; Green – r = 0.25; Blue – r = 0.50; Violet – r = 1.00.

Because we know have a formula for $[(dT)_{18}]$, and we know that

$$-\frac{d[(dT)_{18}]}{dI_a} = \frac{1}{9}\left(\frac{d[T <> T]}{dI_a} + \frac{d[6-4]}{dI_a} - \frac{d[T <> T_{rev}]}{dI_a}\right)$$

and because we already multiplied $[(dT)_{18}]$ by 9, if we assume that the formation of dimer is much greater than either 6-4 photoadduct formation or photoreversal of the dimer, we can conclude that the derivative of this fit function will give us the quantum yield of dimerization. If we choose to take the value of the derivative at $I_a = 0$, then we can effectively ignore photoreversal, which relies on the formation of thymine dimer.

The calculated quantum yields based on these initial slopes are listed in table 4.2, and the reported error is based on 95% confidence interval, from the function:

$$\mu = \bar{x} \pm \frac{ts}{\sqrt{n}}.$$

r	0	0.025	0.05	0.10	0.25	0.50	1.00
$\phi_{T<>T}$ x 10^2	2.8±0.2[29]	3.17±0.05	3.12±0.05	3.25±0.05	3.64±0.05	4.40±0.05	4.76±0.05

Table 4.2: Quantum Yield of Dimerization for various ratios of Ag^+ to $(dT)_{18}$.

Like for $(dT)_{18}$, we can convert the absorbance of TMP into a concentration by taking into account the molar absorptivity of 8700 M^{-1} cm^{-1}. However, the kinetics for the dimerization of TMP differ a bit from $(dT)_{18}$ because it takes two TMP to form one T<>T, rather than one $(dT)_{18}$ to form nine T<>T. Therefore we shall consider:

$$-\frac{1}{2}\frac{d[TMP]}{dI_a} = \left(\frac{d[T<>T]}{dI_a} + \frac{d[6-4]}{dI_a} - \frac{d[T<>T_{rev}]}{dI_a}\right)$$

Therefore, by dividing the concentration of TMP by two, we are able to obtain information about the rate of formation of dimer, formation of 6-4 photoadduct, and the loss of dimer from photoreversal. By assuming that the formation of 6-4 photoadduct is much lower than the formation of dimer, and by taking the initial slope once more to overcome any photoreversal, we can calculate the quantum yield of dimerization. For TMP, the data points can be satisfactorily fit by a linear function.

This linear fit function is applied to both TMP systems in Figure 4.10. The fit parameters and quantum yield are listed in Table 4.4, and because the derivative of the function $a + bI_o$ with respect to I_o is just b, calculating the quantum yield is trivial.

r	a x 10^{-5}	b x 10^{-5}	$\phi_{T<>T}$ x 10^{2}
0	3.8081 ± 0.0008	-5.85 ± 0.07	0.00585 ± 7 x 10^{-5}
10	4.10 ± 0.02	-44 ± 2	0.044 ± 0.002

Table 4.3: Quantum Yield of Dimerization and Linear Fit Parameters for TMP

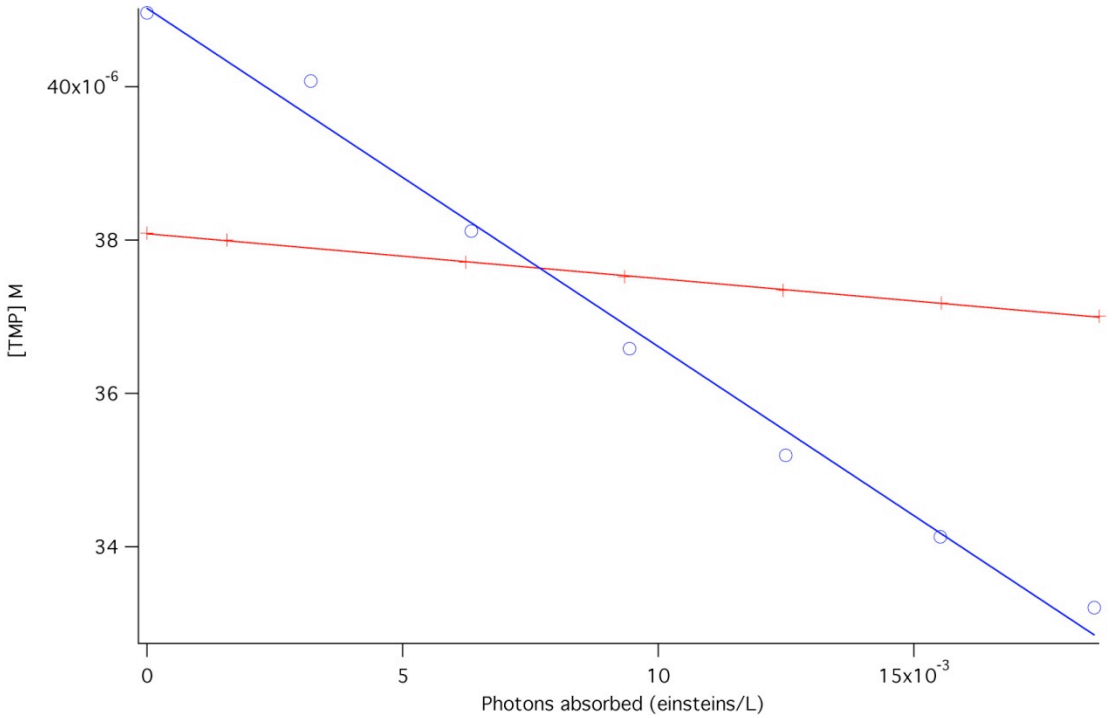

Figure 4.10: Concentration TMP versus photons absorbed, with best fit function imposed. Red – *r* = 0 ; Blue – *r* = 10.

4.1.2 Discussion

The rate of dimerization does not appear to increase until the ratio of Ag+ to nucleic phosphate reaches *r* = 0.25. However, the increase from *r* = 0.025 to *r* = 0.25 is only about 10%. The increase from *r* = 0.25 and *r* = 0.50 is about 20%, and the increase from *r* = 0.50 to *r* = 1.00 is also about 10%. Therefore, the maximum contribution to enhancing dimerization contribution seems to occur during the formation of the Ag+-DNA complex II described by Arakawa et al.[22]

In addition, the rate of dimerization increases almost eight-fold when the ratio of Ag+ to nucleic phosphate in TMP is 10. However, the development of a band between 300 nm and 400 nm that does not appear to be the formation of 6-4 photoproduct is concerning. Further experiments need to be done in order to determine the origin of the chromophore that is generating the band. Perhaps by investigating anaerobic conditions for this system, it may be possible to further enhance thymine dimerization.

4.2 CD spectroscopy

The results of CD spectroscopy indicate the degree of base stacking in the $(dT)_{18}$ system.

4.2.1 Results

The concentration of $(dT)_{18}$ was approximately 5.51×10^{-6} M, although the addition of $AgNO_3$ solution will cause a slight, negligible decrease in concentration throughout the experiment. Although measurements were made in ΔA for each sample, using the built in software, Δε could quickly be calculated for the entire spectrum. The peaks and troughs, along with their related Δε are reported in Table 4.4, and the collected Δε spectra for the various ratios of Ag^+ are shown in Figure 4.11.

r	0	0.025	0.05	0.10	0.25	0.50	1.00
Peak 275 nm Δε (M^{-1} cm^{-1})	72.3	70.1	68.8	70.8	70.2	61.8	52.8
Trough 250 nm Δε (M^{-1} cm^{-1})	-54.1	-52.1	-52.1	-48.1	-49.3	-51.5	-50.3

Table 4.4: Δε for peaks and troughs of CD spectra for given *r* values.

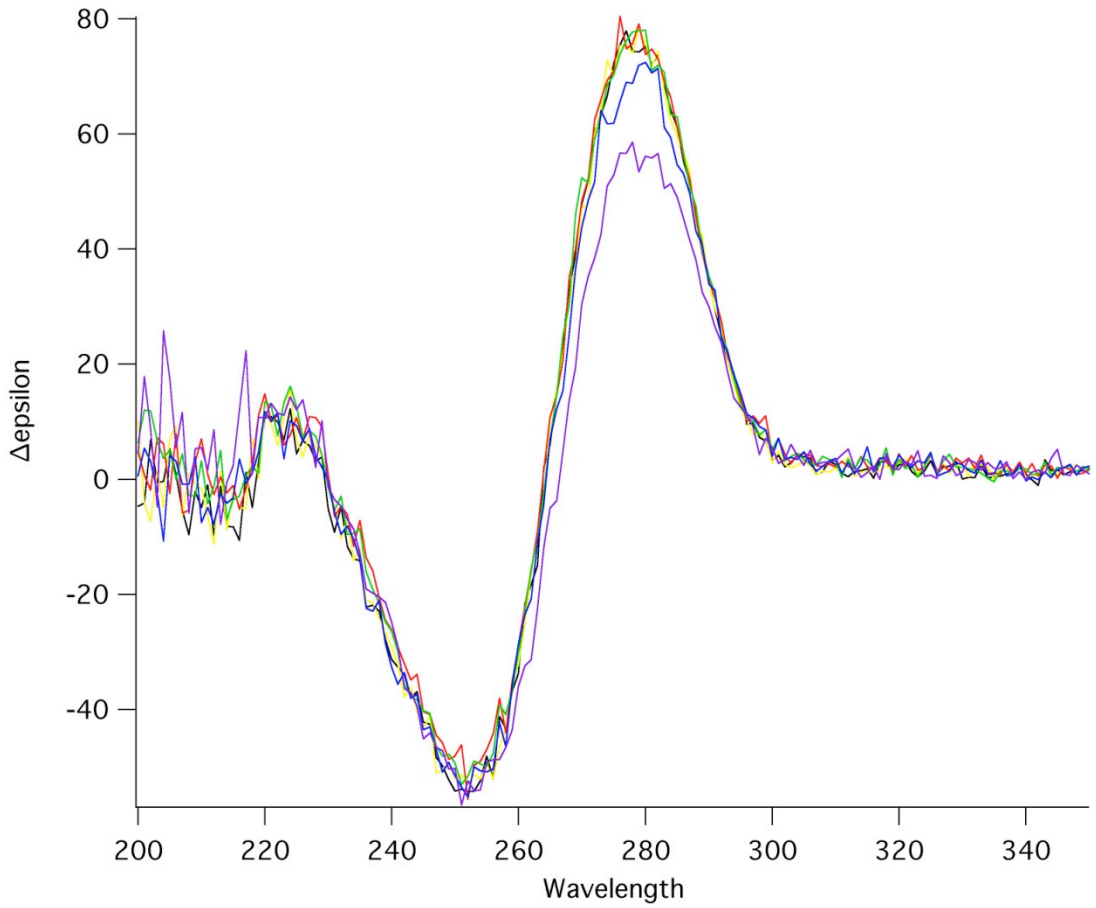

Figure 4.11: Δε versus wavelength in nm. Black – r = 0.00; Red – r = 0.10 ; Orange – r = 0.05; Yellow – r = 0.025; Green – r = 0.25; Blue – r = 0.50 ; Violet – r = 1.00.

4.2.2 Discussion

It is interesting to note that while the Δε at 275 nm decreases when r = 0.5 and 1.0, the Δε at 250 nm does not show significant change throughout the experiment. This may indicate that only the bases are separating due to the presence of Ag^+, which would reduce the strength of the induced CD in the thymine bases. If this explanation is correct, the Δε should continue to decrease until the $(dT)_{18}$ structure is saturated with Ag^+.

Chapter 5
Conclusions

If Ag^+ truly increases intersystem crossing in thymine, then it is predicted that by using femtosecond absorption spectroscopy there should be an observable increased intensity in the amount of $^3\pi\pi^*$ present when pumping at 267 nm and probing at 450 nm. In addition, bleach recovery experiments should show a decrease in the apparent lifetime of the $^1n\pi^*$ state because more energy is being diverted by intersystem crossing.

More work needs to be done in order to attempt to quantify increases to quantum yield of dimerization, specifically by looking into higher values of *r* for $(dT)_{18}$ in order to determine whether Ag^+ can continue to enhance dimerization until Complex III forms, or even after.

It may also be interesting to examine this enhanced quantum yield of dimerization from a clinical point of view to determine if there is any correlation between human exposures to Ag^+ and the risk of developing melanoma.

Bibliography

[1] Cui, R.; Widlund, H. R.; Feige, E.; Lin, J. Y.; Wilensky, D. L.; Igras, V. E.; D'Orazio, J.; Fung, C. Y.; Schanbacher, C. F.; Granter, S. R. *Cell.* **2007**, *128*, 853-864.

[2] Sparling, B. *NAS Educational Resources*. **2001**, http://www.nas.nasa.gov/About/Education/Ozone/ozonelayer.html, (May 5, 2009).

[3] *National Cancer Institute, U.S. National Institutes of Health*. **2004**, http://www.cancer.gov/newscenter/tip-sheet-tanning-booths, (May 5, 2009).

[4] *Cancer Epidemiology in Older Adolescents & Young Adults.* **2007**, SEER AYA Monograph pages *53-57.*

[5] Schreier, W. J.; Schrader, T. E.; Koller, F. O.; Gilch, P.; Crespo-Hernandez, C. E.; Swaminathan, V. N.; Carell, T.; Zinth, W.; Kohler, B. *Science*. **2007**, *315,* 625-629.

[6] Law, Y. K.; Azadi, J.; Crespo-Hernández, C.E.; Olmon, E.; Kohler, B. *Biophysical Journal.* **2008**, *94*, 3590-3600.

[7] Rahn, R. O.; Landry, L. C. *Photochemistry and Photobiology*. **1973**, *18*, 29-38.

[8] Zinchenko, A.; Baigl, D.; Chen, N.; Pyshkina, O.; Endo, K. *Biomacromolecules*. **2008**, *9*, 1981-1987.

[9] Voet, D.; Voet, J. *Biochemistry*; Wiley: New York, Third ed. 2004.

[10] Mouret, S.; Baudouin, C.; Chaveron, M.; Favier, A.; Cadet, J.; Douki, T. *Proceedings of the National Academy of Sciences*. **2006**, *103*, 13765-13770.

[11] Fisher, G. J.; Johns, H. E. *Photochemistry and Photobiology of Nucleic Acids*; Academic Press: New York, Vol 1, 1976, 225-294.

[12] Lee, J. H.; Bae, S. H.; Choi, B. S. *Proceedings of the National Academy of Sciences*. **2000,** *97,* 4591-4596.

[13] Eisinger, J.; Shulman, R. G. *Proceedings of the National Academy of Sciences*. **1967**, *58*, 895-500.

[14] Coons, M. Private correspondence dated 5/05/2009.

[15] Frank, J. K.; Paul, I. C. *Journal of American Chemical Society*. **1973**, *95,*2324-2332.

[16] Cadet, P.; *Bioorganic Photochemistry*; Wiley, New York, 1990.

[17] Hare, P. M.; Crespo-Hernández, C.E; Kohler, B. *Proceedings of the National Academy of Sciences*. **2007**, *104*, 435-440.

[18] Pecourt,J.; Peon, J.; Kohler, B. *Ultrafast Phenomena*. **2000**, 553-555.

[19] Hare, P. M.; Crespo-Hernández, C.E; Kohler, B. *Journal of Physical Chemistry B*. **2006,** *110*, 18641-18650.

[20] Perun, S.; Sobolewski, A.; Domcke, W. *Journal of Physical Chemistry A*. **2006,** *110,* 13239-13244.

[21] Middleton, C.; de La Harpe, K.; Su, C.; Law, Y. K.; Crespo-Hernández, C.E; Kohler, B. *Annual Review of Physical Chemistry*. **2009**, *60*, 217-239.

[22] Arakawa, H.; Neault, J.; Tajmir-Raiahi, H. *Biophysical Journal*. **2001**, *81,* 1580-1587.

[23] Berova, N.; Nakanishi, K.; Woody, R. *Circular Dichroism*; Wiley-VCH: New York, Second ed. 2000.

[24] Tinoco, I.; Sauer, K.; Wang, J.; Puglisi, J. *Physical Chemistry. Principles and Applications in Biological Sciences*; Prentice Hall: New Jersey, Fourth ed. 2002.

[25] El-Sayed, M. A.; *J Chem Phys*. **1962**, *36*, 573-574.

[26] Mouret, S.; Baudouin, C.; Charveron, M.; Favier, A.; Cadet, J.; Douki, T. *Proceedings of the National Academy of Sciences*. **2006,** *103*, 13765-13770.

[27] Douki, T.; Reynaud-Angelin, A.; Cadet, J.; Sage, E. *Biochemistry.* **2003**, *42*, 9221-9226.

[28] Cavaluzzi, M. J.; Borer, P. N. *Nucleic Acids Research*. **2004,** *32*, e13.

[29] Marguet, S.; Markovitsi, D. *J. Am. Chem. Soc.* **2005**, *127*, 5780.